INVESTIGATION OF SINGULARITIES AND SELF-MOTIONS OF THE 3-UPU ROBOT

A. Wolf and M. Shoham
Robotics Laboratory
Department of Mechanical Engineering
Technion – Israel Institute of Technology
http://robotics.technion.ac.il
[alonw,shoham]@tx.technion.ac.il

F.C. Park
School of Mechanical and Aerospace Engineering
Seoul National University
http://robotics.snu.ac.kr
fcp@plaza.snu.ac.kr

Abstract We investigate the singular configurations and self-motion phenomena of the 3-UPU robot. Drawing principally upon tools from line geometry and screw theory, we first derive, as a set of six lines, the 6X6 transformation matrix mapping external wrenches acting on the moving platform to the internal forces/moments of the moving platform's joints. The closest linear complex to these six governing lines is then obtained. The linear complex's axis and pitch not only provide additional information and understanding on the type and location of the singularities, but also on the nature of any instantaneous motions arising from manufacturing tolerances and low rigidity. It is found that at the home position of certain 3-UPU architectures, the corresponding lines are contained in two zero-pitch linear complexes, causing an instantaneous two-parameter rotational motion about a line pencil at the intersection point of the 3-UPU's limbs. In the vicinity of the home position the lines are contained in two close linear complexes, offering a theoretical explanation of the observed sensitivity of this mechanism to manufacturing tolerances.

Keywords: Parallel robot, 3-UPU, singularity, self motion, line geometry.

1. Introduction

The three DOF 3-UPU parallel mechanism, first introduced in the literature by Tsai (1996), has recently been the subject of kinematic analysis by several researchers (Di Gregorio and Parenti-Castelli 1998, 1999, Tsai and Joshi 2000). Yet, it was only at the 2001 Computational Kinematics Workshop in Seoul that F.C. Park demonstrated with a working prototype what looked like a singular or a self motion behavior of the 3-UPU robot. Di Gregorio and Parenti-Castelli (1998) had predicted a limited form of this behavior of the mechanism. The authors pointed out that while in some singular configurations the 3-UPU mechanism has, at least locally, more than three DOF (Degrees of Freedom), meaning that though designed to have three pure translational DOF, the mechanism gains extra uncontrollable rotational DOFs. Yet, it was apparent from the hardware demonstrations that the self-motions were in fact global in nature, occurring over a continuous and arbitrary range of leg lengths. The velocity equation-based analysis presented in Di Gregorio and Parenti-Castelli (1999) predicted the existence of two groups of singularities, termed translational and rotational, for the general 3-UPU mechanism, but as before this was limited to a finite set of configurations. Zlatanov, Bonev, and Gosselin (2001) also verify that the demonstrated 3-UPU architecture is in a singular configuration at the home position.

The present investigation suggests a different approach to the singularity analysis of parallel robots, which not only determines the singular configurations, but also predicts the mechanism behavior near these configurations. Our approach utilizes line geometry to obtain a 6X6 matrix of the robot's governing lines, and then applies an algorithm presented by Pottmann et al. (1999) to find the closest linear complex to this set of six lines, in a given position of the robot. When the six lines are contained in a linear complex, the robot is in a singular configuration and the possible self motion is determined by the linear complex's direction and pitch. The lines may be contained in two or three different linear complexes; in this case the self motions are respectively defined by a two or three parameter motion. Also, sensitivity to manufacturing tolerances can be evaluated by the closeness of the linear complex to the set of lines. This method is demonstrated for the 3-UPU robot.

2. Linear Complex Approximation Algorithm

Given k lines $L_i = (l_i, \bar{l}_i)$, $i = 1, \ldots, k$ $(k \geq 6)$ by their Plücker coordinates, the algorithm finds among all linear complexes the closest one, denoted by C, to this given set of lines L_i. These linear complexes will be denoted by $X = (x, \bar{x}) \in \Re^6$. According to Klein (1921), the moment of a line L with respect to a linear complex X is given by

$$m(L, X) = \frac{|\bar{x} \cdot l + x \cdot \bar{l}|}{\|x\|} \tag{1}$$

Hence, one can compute C as a minimum of

$$\sum_{i=1}^{k} m(L_i, X)^2 \tag{2}$$

among all linear complexes X, given by $X = (x, \bar{x}) \in \Re^6$. This is equivalent to minimizing the positive semidefinite quadratic form

$$F(X) = \sum_{i=1}^{k} \left(\bar{x} \cdot l_i + x \cdot \bar{l}_i\right)^2 = X^T M X \tag{3}$$

under the normalization condition $1 = \|x\|^2 = X^T D X$, where $D = \mathrm{diag}(1,1,1,0,0,0) = \Gamma$, and M is the Gramian matrix. Defining L in axis coordinates as $L_{A,i} = (\bar{l}_{a,i}, l_{a,i})$, M is then the Gramian matrix defined as

$$M = \sum_{i=1}^{k} L_{Aj} \cdot L_{Aj}^T \tag{4}$$

The solution of (3) is a general eigenvalue problem. Using Lagrange multipliers λ, one obtains (where λ are the eigenvalues and X the eigenvectors)

$$(M - \lambda D)X = 0, \quad X^T D X = 1 \tag{5}$$

Hence, λ is the root of the equation

$$\det(M - \lambda D) = 0 \tag{6}$$

For any root λ and corresponding eigenvector $X = (x, \bar{x})$ we have

$$F(X) = X^T M X = \lambda X^T D X = \lambda \tag{7}$$

where all roots are nonnegative and the solution for the linear complex, C, is an eigenvector corresponding to the smallest eigenvalue λ. Given the lines $L_{A,i} = (\bar{l}_{a,i}, l_{a,i})$ and the linear complex C, the standard deviation of the lines from C is given by $\sigma = \sqrt{\lambda/(k-5)}$. Moreover, given the closest linear complex C, its axis A and pitch p are given by $(a, \bar{a}) = (c, \bar{c} - p \cdot c)$ and $p = c \cdot \bar{c}/c^2$, respectively.

When solving Equation 6 two small eigenvalues may appear, meaning that there are two nearly equally good solutions for C, (C_1, C_2). Hence the lines $L_{A,i}$ can be well approximated by the lines of the intersection of the two linear complexes $C_1 \cap C_2$ (this is a two-parameter family of lines—a linear congruence). Analogously, three small eigenvalues $\lambda_1, \lambda_2, \lambda_3$ define three linear complexes (a bundle of complexes). The intersection forms a one-parameter family of lines such as a regulus, a pair of lines, a union of lines or a whole plane.

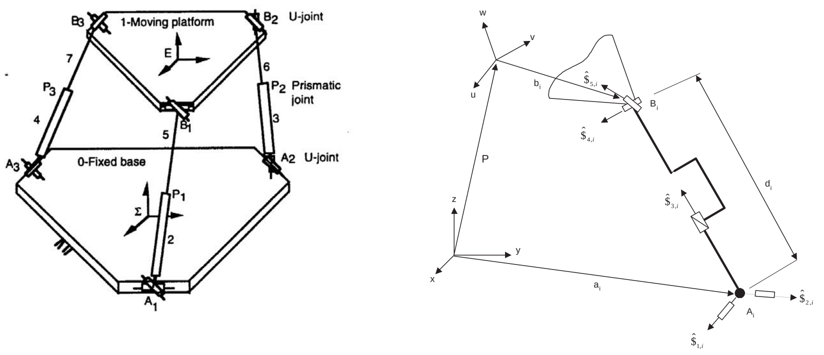

(a) 3-UPU robot (Tsai 1996).

(b) Equivalent limb structure.

Figure 1. The 3-UPU robot and its equivalent kinematic structure.

3. Application to the 3-UPU Robot

It has been shown by Hunt (1978), Merlet (1992), and Husty and Karger (1997), that for a parallel robot with $k \geq 6$ (k is the number of lines describing the limbs of the robot), the robot position is singular if and only if the axes of the limbs lie in a linear complex. For the Stewart-Gough platform, the Jacobian matrix of the manipulator is composed of the lines along its limbs (Ciblak and Lipkin 1999, Tsai *et al* 2000). When a wrench is applied along L_i, $i = 1, \ldots, 6$, then the smallest λ_i produces the least amount of power for a given instantaneous motion. When the reciprocal product is zero, then there is no power generated by the wrenches on the respective twist axis. We use these facts to investigate the 3-UPU parallel robot's structure to gain a better understanding of the robot's singularity and self motion.

Consider the 3-UPU robot in Figure 1-a. The Jacobian matrix of the manipulator is composed of the three screws along its limbs. These screws are the reciprocal screws to all the unactuated joint screws in each limb (Tsai 1998, 2000). In order to define the Jacobian matrix, it is necessary to describe all five joint screws of the manipulator. Note that the only actuated joint in each limb is the third one. Let $s_{i,j}$ be a unit vector along the j-th joint axis of the ith limb. Using this, one can denote the five unit screws of each limb as (see Figure 1-b)

$$\hat{\$}_{1,i} = \begin{bmatrix} \hat{s}_{1,i} \\ (b_i - d_i) \times \hat{s}_{1,i} \end{bmatrix}, \; \hat{\$}_{2,i} = \begin{bmatrix} \hat{s}_{2,i} \\ (b_i - d_i) \times \hat{s}_{2,i} \end{bmatrix}, \; \hat{\$}_{3,i} = \begin{bmatrix} 0 \\ \hat{s}_{3,i} \end{bmatrix},$$

$$\hat{\$}_{4,i} = \begin{bmatrix} \hat{s}_{4,i} \\ b_i \times \hat{s}_{4,i} \end{bmatrix}, \; \hat{\$}_{5,i} = \begin{bmatrix} \hat{s}_{5,i} \\ b_i \times \hat{s}_{5,i} \end{bmatrix} \tag{8}$$

where $b_i = PB_i$, $d_i = A_iB_i = d_i s_{3,i}$, and $\hat{\$}_{3,i}$ is a prismatic joint with infinite pitch. When expressing the instantaneous twist of the moving platform in terms ofthe motion screws and regarding each limb and the platform as an open-loop chain, one obtains (Tsai 1998)

$$\$_p = \dot{\theta}_{1,j}\hat{\$}_{1,j} + \dot{\theta}_{2,j}\hat{\$}_{2,j} + \dot{\theta}_{3,j}\hat{\$}_{3,j} + \dot{\theta}_{4,j}\hat{\$}_{4,j} + \dot{\theta}_{5,j}\hat{\$}_{5,j} \tag{9}$$

Since the axis of all passive joints in each limb intersects the line passing through points A_i, B_i, a wrench that is reciprocal to all the motion screws is given by

$$\$_{r3,i} = \begin{bmatrix} s_{3,i} \\ b_i \times s_{3,i} \end{bmatrix} \tag{10}$$

Taking the reciprocal product $\Omega(\cdot,\cdot)$ of both sides of $\$_p$ with $\$_{r3,i}$ one obtains

$$\Omega(\$_{r3,i}\$_p) = \dot{d}_i, \quad i = 1, 2, 3 \tag{11}$$

Writing this for each limb one gets $J_x\dot{x} = J_q\dot{q}$, where

$$J_x = \begin{bmatrix} (b_1 \times s_{3,1})^T & s_{3,1}^T \\ (b_2 \times s_{3,2})^T & s_{3,2}^T \\ (b_3 \times s_{3,3})^T & s_{3,3}^T \end{bmatrix} \tag{12}$$

with J_q the 3×3 identity matrix, $\dot{x} = (\omega_x, \omega_y, \omega_z, v_{px}, v_{py}, v_{pz})$, and $\dot{q} = (\dot{d}_1, \dot{d}_2, \dot{d}_3)$. Taking $\dot{x}$ to be the velocity of a point p on the moving platform, and $\dot{q}$ as the vector of actuator joint rates, one can define the relation using J_x.

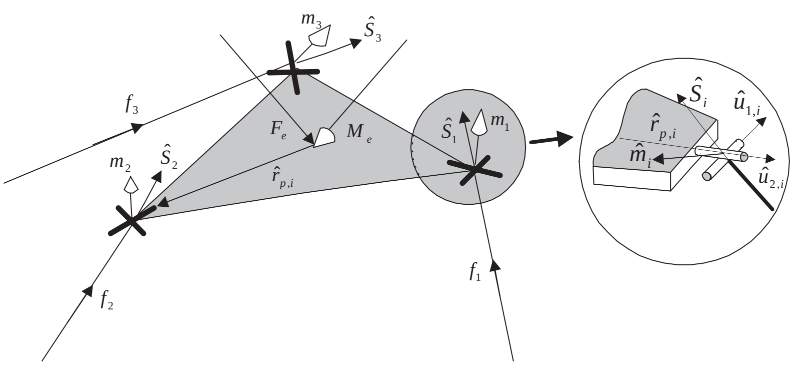

Figure 2. Force and moment transmitted to the moving platform.

The above scheme provides a 3×6 matrix. However, in order to obtain the full 6×6 matrix that maps the external wrench to internal joints' reactions, the static equilibrium of forces and moments about the center of the moving platform has to be derived. These static equilibrium equations are given by (see Figure 2 for definitions)

$$\sum_{i=1}^{3} f_i \hat{s}_i - F_e = 0 \tag{13}$$

$$\sum_{i=1}^{3} m_i \hat{u}_i + \sum_{i=1}^{3} {}^{w}R_P \hat{r}_{p,i} \times f_i \cdot \hat{s}_i - M_e = 0 \tag{14}$$

where $\hat{u}_i$ is a unit vector normal to the two axes of the upper U joint of the limb i, and ${}^{w}R_p$ is a rotation matrix from the platform coordinate system to the reference coordinate system.

Observing Figure 2, $\hat{u}_{2,i}$ is a unit vector along $\hat{r}_p$ (in platform coordinates), $\hat{u}_{1,i}$ is a unit vector along the second pair of the U joint (connected to limb i), and $\hat{s}_i$ is a unit vector along limb i. Due to the U joint structure, $\hat{u}_{1,i}$ is perpendicular to both $\hat{u}_{2,i}$ and $\hat{s}_i$, hence

$$\hat{u}_{1,i} = \frac{\hat{u}_{2,i} \times \hat{s}_i}{|\hat{u}_{2,i} \times \hat{s}_i|} \tag{15}$$

Substituting $\hat{u}_{2,i} =^{w} R_p \hat{r}_{p,i}$ yields

$$\hat{u}_{1,i} =^{w} R_p \hat{r}_{p,i} \times \hat{s}_i \tag{16}$$

Defining

$$\hat{u}_i = \hat{u}_{2,i} \times \hat{u}_{1,i} \tag{17}$$

and substituting (15) and (16) into (17) yields

$$\hat{u}_i =^{w} R_p \hat{r}_{p,i} \times \left(\frac{{}^{w}R_p \hat{r}_{p,i} \times \hat{s}_i}{|{}^{w}R_p \hat{r}_{p,i} \times \hat{s}_i|} \right) \tag{18}$$

The matrix representation of Equations (13) and 14) is given by $GY = B$, where

$$G = \begin{bmatrix} \hat{s}_1 & \hat{s}_2 & \hat{s}_3 & 0 & 0 & 0 \\ {}^{w}R_p \hat{r}_{p,1} \times \hat{s}_1 & {}^{w}R_p \hat{r}_{p,2} \times \hat{s}_2 & {}^{w}R_p \hat{r}_{p,3} \times \hat{s}_3 & \hat{u}_1 & \hat{u}_2 & \hat{u}_3 \end{bmatrix} \tag{19}$$

with $Y = (F_e, M_e) \in \Re^6$ and $B = (f_1, f_2, f_3, m_1, m_2, m_3) \in \Re^6$. Defining $J = G^{-1}$, the forces at the robot's joints are then given by $JY = B$; this result is corroborated by the work of Ciblak and Lipkin (1999), where they developed a model of a rigid body connected to the ground by springs. For the 3-UPU robot, the model consists of three linera springs and three torsional springs in parallel, which resembles J. Observing J, one can see that its columns correspond to lines lying on the *Klein quadric* M_2^4, as they satisfy Klein's equation (Klein 1871, Hunt 1978)

$$p_{01}p_{23} + p_{02}p_{31} + p_{03}p_{12} = 0 \tag{20}$$

3.1 Simulation Results

We now simulate the 3-UPU mechanism using the linear complex approximation algorithm (LCAA) presented above. In the given simulation, the radii of the base and moving platform are $r_b = 25.9806cm$ and $r_p = 20.2072cm$, respectively (as in the real model of Park). The limbs of the robot are equally divided every 120°, both in the base and in the moving platform. The location of the mid moving platform while in the home position is ${}^wP_p = (0, 0, 50)$.

The three axes of the linear complexes as found by the algorithm are:

$$\begin{aligned} A_1 &= (-0, 9382, 0, 346, 0, -34.5987, -93.8239, 0) \\ A_2 &= (0.346, 0.9382, 0, -93.8239, 34.5987, 0) \\ A_3 &= (0, 0, 1, 0, 0, 0) \end{aligned}$$

where $\lambda_1 = \lambda_2 = \lambda_3 = 0$. Using (refeqn:Sr3i) one obtains $\sigma_1 = \sigma_2 = 0$ and $\sigma_3 = 1.7321$, and the corresponding pitches are all zero.

3.2 Discussion

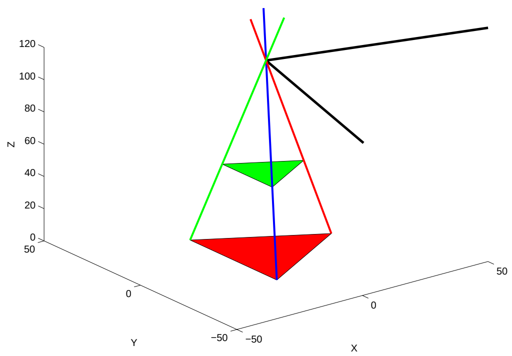

Figure 3. 3-UPU: two zero-pitch linear complexes.

Applying the method of the closest linear complex on the 3-UPU robot in its zero position $P = (0, 0, p_z)$, the lines of J are contained in two zero-pitch linear complexes C_1 and C_2, passing at the intersection point of the extension of the three limbs of the actuator (see the black lines in Figure 3). The intersection of $C_1 \cap C_2$ defines a two-parameter family of lines: a congruence. This result implies that the robot gains an instantaneous two-parameter rotational motion about any horizontal axes passing through the intersection point of the robot's limbs. These axes are the linear combination of the two zero-pitch screws as they define a plane pencil whose vertex is the intersection point of the limbs.

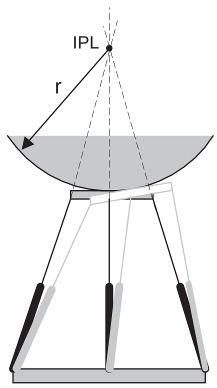

Figure 4. Platform at zero position and at points on a sphere centered at the IPL.

When the robot moves in the vicinity of its base configuration (Figure 4), then it is no longer in a singular configuration. Observing equations (7), one can see that λ has the meaning of the sum of squares of the mutual moment of the lines L_i with respect to C. Hence, σ can be interpreted as the sum of the squares of errors from L_i to C. Moreover, observing the definition of the pitch of the closest linear complex, one can observe that p has a meaning of the projection of the moment of C on a unit screw along C. Hence, the moment m, the STD σ, and the pitch p are distances in Euclidean geometry. Therefore, all results ofthe LCAA must be analyzed relative to the object dimension and the error tolerances utilized during manufacturing. This means that even if for nonsingular configuration, for low values of σ (smaller than error tolerances), the robot may still rotate around the intersection point of the limbs (IPL) uncontrollably.

The following simulation presents motion of the robot on a sphere centered at the original intersection of the limbs, and at each point the LCAA has been applied. It can be seen that the robot is no longer in a singular position. However, there are still two linear complexes with low values of σ. According to measurements taken on Park's prototype, the robot had a self-motion within a radius of approximately 14 cm from the

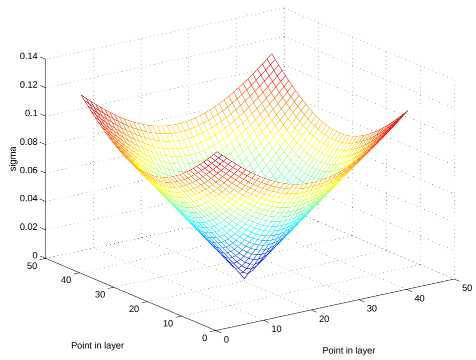

Figure 5. The two minimum σ (rigidity) values corresponding to the two LC axes of Figures 3, 4.

home position. According to the given simulation (Figure 5), σ value within this region attain a maximum value of 0.05 and a minimum of 0 (in centimeters). These results, together with the distance meanings of λ, σ, and p, point to a possibility of an uncontrolled motion of the platform as was observed.

4. Conclusions

In this investigation, the self-motions of the 3-UPU manipulator as was presented by F.C. Park at Computational Kinematics 2001 in Seoul is analyzed. Investigation of the 6×6 Jacobian matrix J of the 3-UPU manipulator in its home position reveals that the matrix is singular. Moreover, by using the linear complex approximation method it has been shown that the lines of J are contained in two axes of two zero-pitch linear complexes (linear congruence). This result implies that the robot gains an instantaneous mobility of two-parameter motion. This motion is a pure rotation about any screw axis, which belongs to the flat pencil, defined by the two axes of the linear complexes. Moreover, when the robot moves along a sphere centered at the initial limb intersection point, it is no longer at a singular point, yet J is still close to two linear complexes with low values of σ. This might still allow for two uncontrolled motions of the moving platform due to manufacturing tolerances or low rigidity, which points to the sensitivity of this mechanism design. In a related paper (Han *et al* 2002), the contribution of the universal joints' torsional clearance to self-motions is analyzed. We believe a comprehensive analytical description of the self-motion phenomenon still remains a topic of further investigation.

References

Han, C.H., Kim, Jinwook, Kim, Jongwon, and Park, F.C. (2002), Kinematic sensitivity analysis of the 3-UPU parallel mechanism, *Mechanism and Machine Theory* (to appear).

Ciblak N., and Lipkin, H. (1999), Synthesis of cartesian stiffness for robotic applications, *Proc. 1999 IEEE Int. Conf. Robotics and Automation*, Detroit, Michigan., pp. 2147-2152.

Di Gregorio, R. and Parenti-Castelli, V. (1998), A translational 3-DOF parallel manipulator, *Advances in Robot Kinematics: Analysis and Control*, J. Lenarcic and M. L. Husty (eds), Dordrecht, Kluwer, pp. 49-58.

Di Gregorio, R. and Parenti-Castelli, V. (1999), Mobility analysis of the 3-UPU parallel mechanism assembled for a pure translational motion, *Proc. IEEE/ASME Int. Conf. Advanced Intelligent Mechatronics*, Atlanta, GA, Sept. 19-23, pp. 520-525.

Hunt, K.H (1983), Structural kinematics of in-parallel actuated robot arms, *ASME J. Mechanisms, Transmissions and Automation in Design*, no. 4, vol. 105, pp. 705-712.

Karger, A., and Husty, M. (1996), On self-motions of a class of parallel manipulators, *Advances in Robot Kinematics*, J. Lenarcic and V. Parenti-Castelli (eds), Dordrecht, Kluwer, pp. 339-348.

Klein F. (1921), *Die Allgemeine Lineare Transformation der Linienkoordinaten*, Gesammelte math. Abhanlungen I, Berlin, Springer.

Merlet, J.P. (1992), Singular configurations of parallel manipulators and grassmann geometry, *Int. J. Robotics Research*, no. 5, vol. 8, pp. 45-56.

Pottmann, H., Peternell, M., and Ravani, B. (1999), An introduction to line geometry with applications, *Computer Aided Design*, vol. 31, pp. 3-16.

Pottmann H., Wallner, J. (2000), *Computational Line Geometry*, Springer, Berlin.

Tsai, L-W. (1996), Kinematics of a three-DOF platform with three extensible limbs, *Recent Advances in Robot Kinematics,* J. Lenarcic and V. Parenti-Castelli (eds.), Dordrecht, Kluwer, pp. 401-410.

Tsai L-W. (1998), The Jacobian analysis of a parallel manipulator using reciprocal screws, *Advances in Robot Kinematics: Analysis and Control,* J. Lenarcic, and M.L. Husty, (eds), Dordrecht, Kluwer, pp. 327-336.

Tsai, L-W., and Joshi, S. (2000), Kinematics and optimization of a spatial 3-UPU parallel manipulator, *ASME J. Mechanical Design*, pp. 439-446.

Zlatanov D., Bonev, L., and Gosselin, C. (2001), Constraint Singularities, *NewsLetter on: http://www.parallemic.org*, July.